Design and Analysis of Compact Self-Multiplexing Antenna Based on Half-Mode Substrate-Integrated Circular and Rectangular Cavities

Rusan Kumar Barik*(1), Rathod Rajender(2), Xiaoguang Liu(1), and Daniele Rossi(2)
(1) School of Microelectronics, Southern University of Science and Technology, Shenzhen, China
(2) Department of Information Engineering, University of Pisa, 56126 Pisa, Italy

Abstract

This paper presents the design and analysis of a compact self-multiplexing antenna (SMA) for pentaband applications. The proposed antenna is built using half-mode (HM) substrate-integrated circular and rectangular cavities loaded with slots. The HM circular cavity is excited through three 50 Ω microstrip lines, which facilitate three distinct frequency bands. In contrast, the HM rectangular cavity is activated using two 50 Ω coaxial probes, yielding two different operating frequencies. Thus, the proposed SMA operates at 3.91 GHz (5G band), 4.4 GHz (5G band), 4.99 GHz (5G band), 5.83 GHz (WLAN/WiMAX), and 6.59 GHz (Extended C-band). The radiation process, operating principle, and frequency tunability are explored in depth. The proposed SMA features a compact footprint area of $0.43\lambda_g^2$ and attains an isolation level exceeding 24.5 dB. The antenna achieves realized gains of 3.46 dBi, 3.23 dBi, 3.44 dBi, 5.19 dBi, and 4.23 dBi, along with efficiencies exceeding 82%, 87%, 92%, 71%, and 90% at frequencies of 3.91 GHz, 4.4 GHz, 4.99 GHz, 5.83 GHz, and 6.59 GHz, respectively.

1 Introduction

The rapid advancement of modern wireless systems necessitates compact multi-band antennas, as they inherently eliminate the need for multiple single-band antennas for operations across various frequencies [1-5]. However, these multi-band antennas, which operate at different frequencies, experience poor isolation and high interference. To improve isolation and reduce interference, it is necessary to incorporate additional frequency selective devices like diplexers or triplexers rather than multiplexers. Nonetheless, this extra device contributes to an increase in circuit area, cost, and design complexity.

In recent years, various self-diplexing, self-triplexing, and self-quadruplexing antennas have been developed to eliminate the need for additional multiplexer circuits, demonstrating excellent isolation while significantly reducing footprint area [6-11]. In [6-7], self-diplexing antennas that are highly miniaturized, utilizing half-mode (HM) and quarter-mode (QM) substrate-integrated cavities (SICs), are proposed to attain high isolation and frequency reconfigurability. A compact self-triplexing antenna is designed in [8] using a SIC loaded with a T-shaped slot and square-loop for Ku-band communication. A self-quadruplexing slot antenna utilizing a square cavity with four T-shaped slots is introduced to attain circularly polarized frequency bands in [9]. A self-diplexing antenna is developed in [10], utilizing a square SIC cavity and half-mode resonators to function at microwave and mm-wave frequencies. A highly compact self-quadruplexing antenna is constructed using a substrate-integrated rectangular cavity that incorporates two U-shaped slots, resulting in exceptionally high isolation. Further study is necessary for the advancement of compact self-multiplexing antennas that exhibit high isolation and are resistant to interference.

This paper presents the design and analysis of a compact self-multiplexing antenna (SMA) intended for pentaband applications. The proposed antenna is designed using half-mode circular and rectangular cavities that are equipped with slots. The design stages are elaborated upon, along with the working principle, radiation mechanism, and parametric analysis. The proposed antenna demonstrates an isolation exceeding 24.5 dB while maintaining a compact footprint area of $0.43\lambda_g^2$.

2 Design and Analysis of SMA

2.1 Antenna Configuration

The configuration of the proposed self-multiplexing antenna (SMA) is illustrated in Fig. 1. The proposed SMA structure is built by using circular and rectangular half-mode (HM) cavities which are realized on a Rogers 4003C substrate with thickness of 0.813 mm, dielectric constant of 3.38, and dissipation factor of 0.0021. The rectangular HM cavity is embedded in the circular HM cavity. The circular HM cavity is excited by applying three 50Ω microstrip lines which provides three resonant frequencies, whereas the rectangular HM cavity is excited by using two 50Ω coaxial probes to achieve two different frequency bands. By using the HM cavities, the size of the proposed SMA is reduced by 50% and further miniaturization is achieved due to the capacitive loading produced by the slots. The formation of HM cavities and step-by-step design stages are depicted in Figs. 2 and 3, respectively. Initially, a full-mode

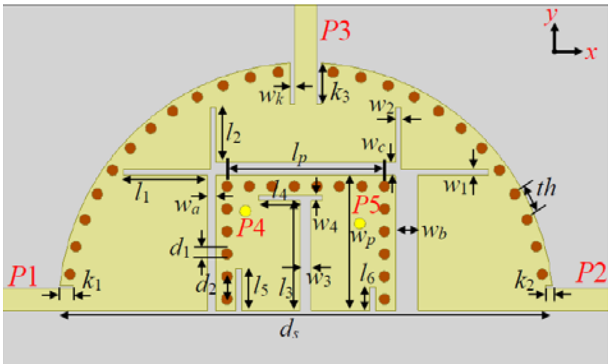

Figure 1. Proposed self-multiplexing antenna. Final dimensions (unit: mm): $d_s = 44.0$, $l_p = 14$, $w_p = 12$, $l_1 = 7.05$, $w_1 = 0.5$, $l_2 = 5$, $w_2 = 0.5$, $w_a = 1.2$, $w_b = 2.5$, $w_c = 1.6$, $l_3 = 9.7$, $l_4 = 3.7$, $l_5 = 4.8$, $l_6 = 2.08$, $w_3 = 1$, $w_4 = 0.5$, $k_1 = 1.3$, $k_2 = 0.7$, $k_3 = 3.7$, $w_k = 0.211$, $d_1 = 1.0$, $d_2 = 2.0$, $th = 6.9$.

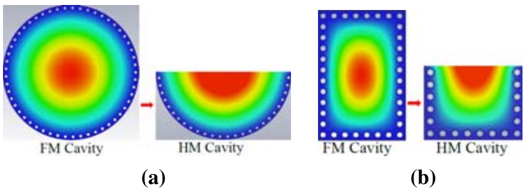

Figure 2. Generation of half-mode resonators form the full-mode cavities: (a) Circular; (b) Rectangular.

circular cavity (diameter = 44 mm) and rectangular cavity (14 mm $\times$ 22 mm) operating at TM_{010} and TE_{110} modes, respectively, are divided horizontally to form the half-mode cavities as illustrated in Fig. 2.

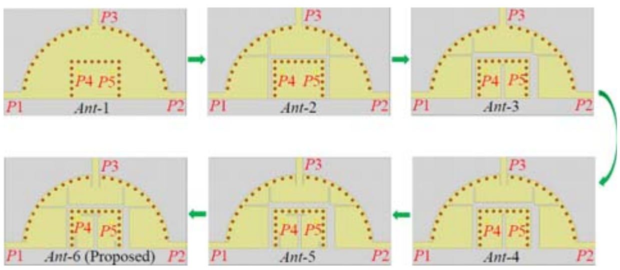

Figure 3. Step-by-step design stages.

The proposed SMA is realized using a step-by-step design process as shown in Fig. 3. Ant-1 is developed by embedding the rectangular HM cavity in the circular HM cavity and applying the excitations using three 50 Ω microstrip lines and two 50 Ω coaxial probes. The full-wave S-parameters of the Ant-1 are shown in Fig. 4(a). From the figure, it can observed that the semi-circular cavity resonates at 6.6 GHz (port-1 and port-2 have same frequency) and 9.17 GHz (port 3) and provides poor impedance matching whereas the rectangular cavity resonates at 7.05 GHz (port-4 and port-5 have the same frequency). Next, one horizontal slot and two vertical slots are engraved on the top plane to form the Ant-2. The EM simulated S-parameters of Ant-2 is depicted in Fig. 4(b). Due to the slots, the ca-

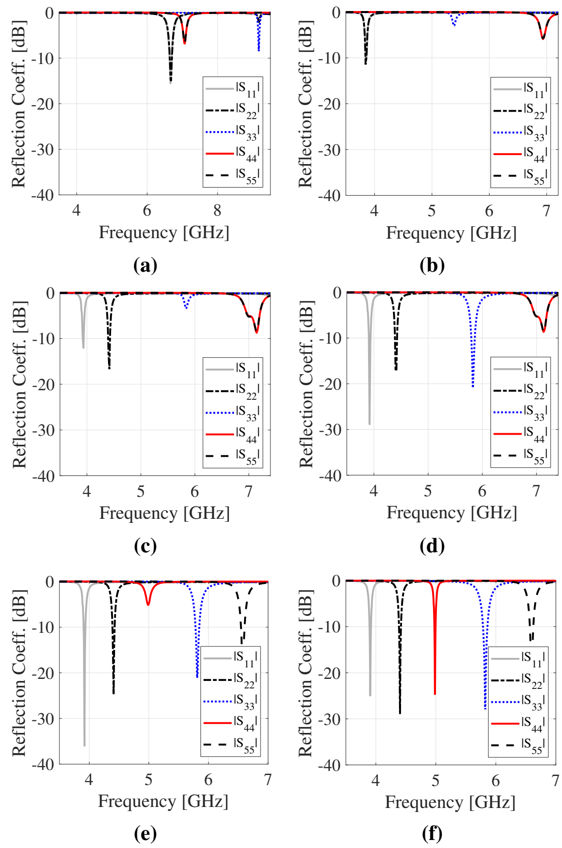

Figure 4. Reflection coefficients of the various design stages. (a) Ant-1; (b) Ant-2; (c) Ant-3; (d) Ant-4; (e) Ant-5; and (f) Ant-6.

pacitive loading on the cavity increases, which results in shifting of resonating frequencies. The ports 1 and 2 resonate at 3.9 GHz, whereas the port-3 frequency shifts to 5.39 GHz. To achieve the desired frequency bands, additional slots are added corresponding to ports 1, 2, and 3, thus resulting in the generation of Ant-3. The corresponding reflection coefficients are shown in Fig. 4(c). The resonant frequencies at ports 1, 2, and 3 are 3.91 GHz, 4.4 GHz, and 5.82 GHz, respectively. At the same time the resonant frequencies at ports 4 and 5 remain unchanged. Next, Ant-4 is designed by applying inline feeding technique to achieve the impedance matching at ports 1, 2, and 3. The corresponding S-parameters are depicted in Fig. 4(d), which shows that the reflection coefficients at ports 1, 2, and 3 are better than -15 dB. Subsequently, Ant-5 is realized by adding slots on the rectangular cavity to achieve fourth and fifth resonant frequencies. The full-wave simulated S-parameters are shown in Fig. 4(e). It is found that the resonant frequencies are 4.99 GHz and 6.59 GHz corresponding for ports 4 and 5, respectively. However, the impedance matching at port 4 is poor. Therefore, the location of the coaxial probe corresponding to port-4 is optimized to achieve good impedance matching in final design (Ant-6). The full-wave simulated S-parameters of the Ant-6 is depicted in Fig. 4(f), which provides five resonant frequencies with excellent impedance matching as well as high isolation greater than 24.5 dB. The surface current distribution of the proposed antenna at individual ports are depicted in Fig. 5.

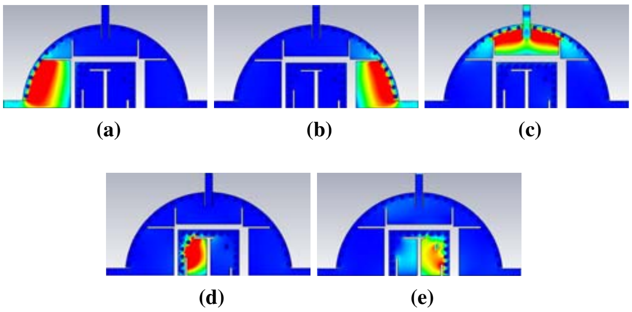

Figure 5. Surface current distribution at individual ports. (a) At 3.91 GHz (Port 1 in ON); (b) at 4.4 GHz (Port 2 is ON); (c) At 5.83 GHz (Port 3 in ON); (d) at 4.99 GHz (Port 4 is ON); (e) at 6.59 GHz (Port 5 is ON).

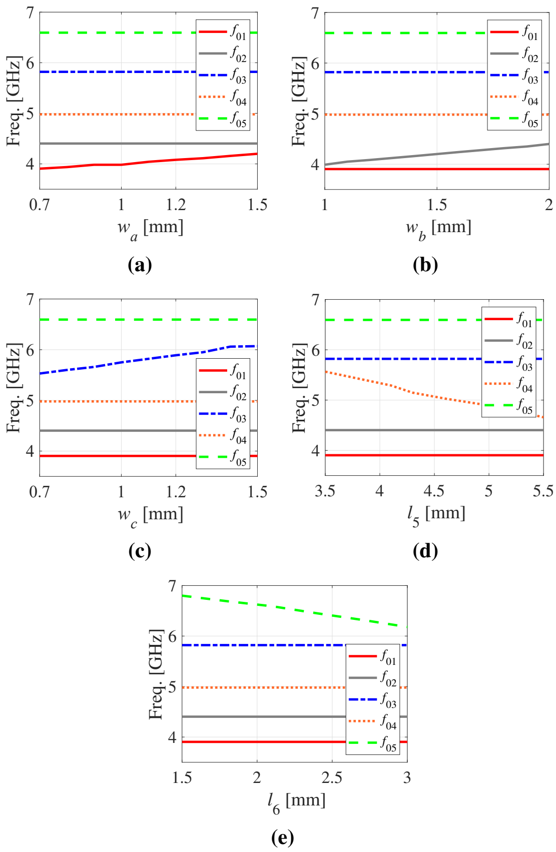

Figure 6. Tunability of resonating frequencies: (a) f_{01}, (b) f_{02}, (c) f_{03}, (d) f_{04}, and (e) f_{05}.

2.2 Frequency Tunability

One important performance metric for the suggested SMA is the frequency bands' independent tunability. By altering the dimensions of the slots that correspond to various ports, frequency tunability is accomplished. The effective capacitive loadings on the cavities change as the slot size are changed, which raises or lowers the particular frequency bands. The tuning of certain frequency bands is shown in Fig. 6. It is evident from Fig. 6(a) that the initial resonant frequency may be changed from 3.9 GHz to 4.2 GHz by changing the parameter w_a from 0.7 mm to 1.5 mm, without impacting other frequencies. Without changing any other frequency bands, the second operational band fluctuated from 3.99 GHz to 4.4 GHz when the parameter w_b changed from 1.0 mm to 2.0 mm, as shown in Fig. 6(b). Similar to this, as shown in Fig. 6(c), the third frequency band may be changed from 5.53 GHz to 6.07 GHz by changing the parameter w_c from 0.7 mm to 1.5 mm without impacting other bands. With reference to Fig. 6(d), it can be seen that the fourth resonant frequency changes from 5.56 GHz to 4.65 GHz while maintaining the other bands when the parameter l_5 is adjusted from 3.5 mm to 5.5 mm. Fig. 6(e) shows that the fifth operational band may be adjusted from 6.8 GHz to 6.18 GHz without changing any other frequency bands when the parameter l_6 is changed from 1.5 mm to 3 mm.

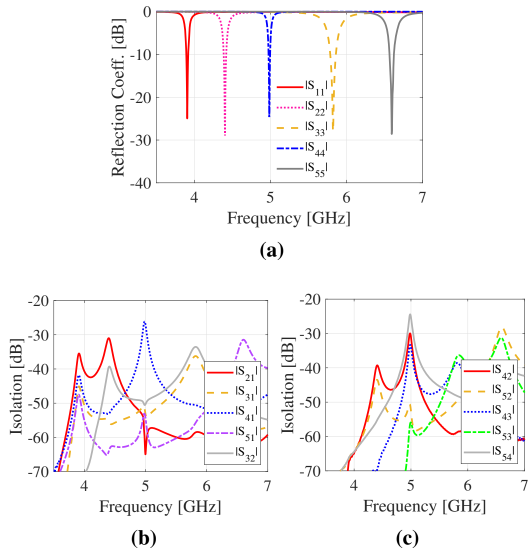

Figure 7. (a) Reflection coefficients, (b) Isolation ($S_{21}/S_{31}/S_{41}/S_{51}/S_{32}$), and (c) Isolation ($S_{42}/S_{52}/S_{43}/S_{53}/S_{54}$) of the suggested SMA.

3 Results and Discussion

A miniaturized SMA based on circular and rectangular half-mode cavities is designed, examined, and optimized for 5G/WLAN/WiMAX/Extended C-band applications in order to validate the aforementioned theoretical idea. The area occupied by the suggested SMA is $0.43\lambda_g^2$. CST Microwave Studio is used to carry out the full-wave simulation. Fig. 7 shows the reflection efficients and isolation of the proposed SMA. From Fig. 7(a), it is seen that the reflection coefficients are better than -24.9, -28.9, -24.6, -27.9, and -28.5 dB at 3.91, 4.4, 4.99, 5.83, and 6.59 GHz, respectively. Looking at Figs. 7(b) and 7(c), it is found that the minimum isolation at 3.91, 4.4, 4.99, 5.83, and 6.59 GHz are obtained as 35.4, 31.1, 24.5, 33.5, and 28.1 dB, respectively.

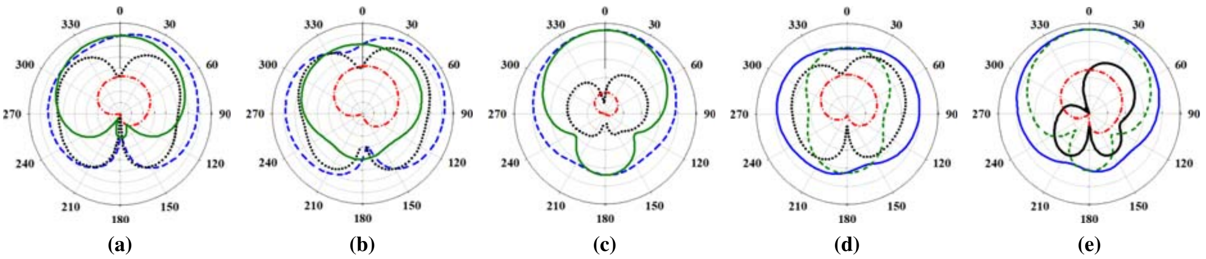

Figure 8. Radiation patterns of the proposed self-multiplexing antenna: (a) At 3.91 GHz (Port 1 in ON); (b) at 4.4 GHz (Port 2 is ON); (c) At 5.83 GHz (Port 3 in ON); (d) at 4.99 GHz (Port 4 is ON); (e) at 6.59 GHz (Port 5 is ON). [E-plane copol (solid); E-plane crosspol (dash-dot); H-plane copol (dash-dash); H-plane crosspol (dot-dot)].

Table 1. State-of-the-arts self-multiplexing antennas

Ref.	Operation	Isolation (dB)	Gain (dBi)	Size (λ_g^2)	SMA
[3]	Quad-band	NA	NA	0.042	×
[4]	Pentaband	NA	NA	0.243	×
[5]	Pentaband	NA	-2 – 1.6	0.713	×
[9]	Quad-band	27	5.2 – 7	1.17	√
[10]	Quad-band	>20	5.22 – 8.7	0.51	√
[11]	Quad-band	>32.5	3.39 – 6.1	0.125	√
Prop.	**Pentaband**	**>24.5**	**3.23 – 5.19**	**0.43**	√

By applying excitation at one port and matching termination at other ports, and vice versa, the far-field antenna performances are captured. The full-wave simulated realized gains are higher than 3.46, 3.23, 3.44, 5.19, and 4.23 dBi and the total efficiencies are calculated to be 82.7%, 87.8%, 71.1%, 92.8%, and 90.1% at frequencies of 3.91, 4.4, 4.99, 5.83, and 6.59 GHz, respectively. Fig. 8 shows the far-field radiation pattern of the proposed SMA. Looking at the Fig. 8, it is observed that the radiation patterns in H-plane ($\phi = 90°$) and E-plane ($\phi = 0°$) are stable and unidirectional. The cross-polarization levels and front-to-back-ratios (FTBR) of the proposed SMA are greater than -14 dB and 16 dB, respectively. The advantageous features of the proposed SMA are compared with the previously reported SMAs and highlighted in Table 1. Compared to existing SMAs, the proposed antenna exhibits five different frequencies with self-multiplexing characteristics as well as high isolation and smaller footprint area.

4 Conclusion

A compact self-multiplexing cavity-backed antenna has been proposed for fifth-generation (5G), wireless LAN (WLAN), Worldwide Interoperability for Microwave Access (WiMAX), and super extended C-band applications. The proposed antenna has been built on the half-mode circular and rectangular cavities with loaded slots. Three 50Ω microstrip feed lines spaced 90° apart are applied for the excitation of half-mode circular cavity to produce three different frequencies, whereas the rectangular HM cavity is excited by using two coaxial 50Ω probes to achieve two distinct frequencies. The working principle, radiation mechanism, and parametric analysis are discussed in detail. The proposed SMA exhibits an isolation greater than 24.5dB with a smaller footprint area of $0.43\lambda_g^2$. Furthermore, the SMA achieves the realized gain of 3.46 dBi, 3.23 dBi, 3.44 dBi, 5.19 dBi, and 4.23 dBi and efficiency greater than 82%, 87%, 92%, 71%, and 90% at 3.91 GHz, 4.4 GHz, 4.99 GHz, 5.83 GHz, and 6.59 GHz, respectively. The manufacturing and experimental demonstration of the proposed SMA are currently in progress.

References

[1] L. Chang and H. Liu, "Low-Profile and Miniaturized Dual-Band Microstrip Patch Antenna for 5G Mobile Terminals," *IEEE Trans. Ant. Propag.*, **70**, 3, March 2022, pp. 2328-2333.

[2] H. Chen, Y. Shao, Y. Zhang, C. Zhang and Z. Zhang, "A Millimeter-Wave Triple-Band SIW Antenna With Dual-Sense Circular Polarization," *IEEE Trans. Ant. Propag.*, **68**, 12, Dec. 2020, pp. 8162-8167.

[3] H. Mopidevi, Y. Damgaci, D. Rodrigo, L. Jofre and B. A. Cetiner, "A Quad-Band Antenna for Public Safety Applications," *IEEE Ant. Wireless Propag. Lett.*, **13**, July 2014, pp. 1231-1234.

[4] I. -F. Chen and C. -M. Peng, "Compact Modified Pentaband Meander-Line Antenna for Mobile Handsets Applications," *IEEE Ant. Wireless Propag. Lett.*, **10**, July 2011, pp. 607-610.

[5] M. G. N. Alsath and M. Kanagasabai, "Planar Pentaband Antenna for Vehicular Communication Application," *IEEE Ant. Wireless Propag. Lett.*, **13**, Jan. 2014, pp. 110-113.

[6] R. K. Barik, X. Wu, X. Liu and S. Koziel, "An Extremely Compact Frequency-Reconfigurable Self-Diplexing Antenna Employing Dielectric Liquids," *IEEE Ant. Wireless Propag. Lett.*, **23**, 11, Nov. 2024, pp. 3749-3753.

[7] R. K. Barik, X. Liu and S. Koziel, "Highly Compact Microfluidically Frequency-Tunable Self-Duplexing Antenna for Sub 6-GHz 5G Applications," *2024 4th URSI Atlantic Radio Science Meeting (AT-RASC)*, Meloneras, Spain, 2024, pp. 1-4.

[8] Y. Yao, G. Dong, Z. Zhu and Y. Yang, "Design of Substrate Integrated Waveguide Cavity-Backed Self-Triplexing Antenna," *IEEE Ant. Wireless Propag. Lett.*, **23**, 2, Feb. 2024, pp. 803-807.

[9] K. Kumar, S. Priya, S. Dwari and M. K. Mandal, "Self-Quadruplexing Circularly Polarized SIW Cavity-Backed Slot Antennas," *IEEE Trans. Ant. Propag.*, **68**, 8, Aug. 2020, pp. 6419-6423.

[10] H. Naseri, P. PourMohammadi, A. Iqbal, A. A. Kishk and T. A. Denidni, "SIW-Based Self-Quadruplexing Antenna for Microwave and mm-Wave Frequencies," *IEEE Ant. Wireless Propag. Lett.*, **21**, 7, July 2022, pp. 1482-1486.

[11] R. K. Barik and S. Koziel, "Highly Miniaturized Self-Quadruplexing Antenna Based on Substrate-Integrated Rectangular Cavity," *IEEE Ant. Wireless Propag. Lett.*, **22**, 3, March 2023, pp. 482-486.